



An instrument for in-situ measurement of total ozone reactivity

Roberto Sommariva¹, Louisa J. Kramer¹, Leigh R. Crilley¹, Mohammed S. Alam¹, and William J. Bloss¹

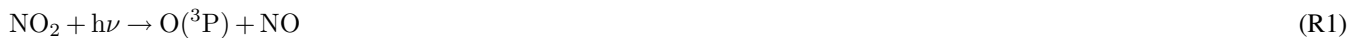
¹School of Geography, Earth and Environmental Sciences, University of Birmingham, Birmingham, UK

Correspondence: R. Sommariva (r.c.sommariva@bham.ac.uk)

Abstract. We present an instrument for the measurement of total ozone reactivity (R_{O_3}), i.e. the reciprocal of the chemical lifetime of ozone (O_3) in the troposphere. The Total Ozone Reactivity System (TORS) was developed with the objective to study the role of biogenic organic compounds (BVOCs) as chemical sinks of tropospheric ozone. The instrument was extensively characterized and tested in the laboratory using individual compounds and small plants (lemonthyme, *Thymus citriodorus*) in a Teflon bag and proved able to measure reactivities corresponding to $> 4.5 \times 10^{-5} \text{ s}^{-1}$, corresponding to 20 ppb of α -pinene or 150 ppb of isoprene in isolation – larger than typical ambient levels but consistent with levels commonly found in environmental chamber and enclosure experiments. The functionality of TORS was demonstrated in quasi-ambient conditions with a deployment in a horticultural glasshouse containing a range of aromatic plants. The measurements of total ozone reactivity made in the glasshouse showed a clear diurnal pattern, following the emissions of BVOCs, and is consistent with mixing ratios of tens ppb of monoterpenes and several ppb of sesquiterpenes.

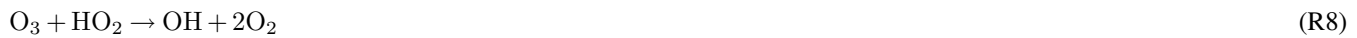
1 Introduction

Ozone (O_3) is a key component of the troposphere: it is known to be damaging for human health and vegetation, to reduce crop yields, and it is an important greenhouse gas (Monks et al., 2015). Ozone is also a primary source of the OH radical, the main atmospheric oxidant, and acts as an oxidant itself (Johnson and Marston, 2008). Because of its importance to tropospheric chemistry, the ozone budget has long been a subject of considerable interest. Ozone is not directly emitted, but is formed in the atmosphere via photolysis of nitrogen dioxide (NO_2), followed by reaction of atomic oxygen with molecular oxygen (R1-R2):



Ozone is destroyed in the troposphere via a series of processes, both physical (e.g., dry and wet deposition) and chemical (Monks et al., 2015). The latter involve photolysis (R3-R4) and reactions with a range of inorganic molecules and unsaturated volatile organic compounds (R5-R9):





Ozone photolysis forms atomic oxygen in ground ($\text{O}({}^3\text{P})$) and excited ($\text{O}({}^1\text{D})$) state and primarily reacts with the molecular oxygen in the atmosphere to reform ozone in a null cycle (R2, R10). However, a small fraction ($\sim 10\%$ in the lower troposphere) of $\text{O}({}^1\text{D})$ reacts with water vapour to form OH radicals (R11), a key process for the oxidative capacity of the atmosphere:



The chemical losses of ozone are one of the least understood parts of the tropospheric ozone budget, in particular because of the many unknowns related to the abundance of volatile organic compounds (VOCs) and their reactivity with ozone (Johnson and Marston, 2008; Glasius and Goldstein, 2016). The organic compounds that react with ozone contain one or more double carbon bonds (e.g., alkenes and dialkenes), and many of these species are emitted by plants during their metabolic processes. These biogenic VOCs (BVOCs) constitute a large fraction of the carbon loading of the atmosphere: estimates suggest that the total biogenic sources of VOCs can be 8-10 times larger than the total anthropogenic sources (Williams, 2004; Glasius and Goldstein, 2016). Isoprene is by far the most important BVOC, accounting for $\sim 50\%$ of the total natural emissions of



non-methane hydrocarbons by mass, followed by monoterpenes (15%), methanol (9%), CO (7%) and a range of other organic compounds which include acetone (4%) and sesquiterpenes (3%) (Guenther et al., 2012).

However, due to the limitations of the analytical techniques used to measure VOCs, it is very likely that both the number and the mass of BVOCs in the troposphere are severely underestimated (Di Carlo et al., 2004; Sinha et al., 2010; Whalley 45 et al., 2011). Estimates vary depending on the approach used, but it is thought that between 20% and 60% (and possibly more) of the total organic carbon pool in the troposphere is currently unaccounted for (Lewis et al., 2000; Goldstein and Galbally, 2007; Glasius and Goldstein, 2016). A significant fraction of these unmeasured organic compounds is constituted by biogenic VOCs: besides isoprene, only a few monoterpenes (e.g., α -pinene, β -pinene, limonene) and even fewer sesquiterpenes (e.g., β -caryophyllene) are routinely measured in the atmosphere (Bouvier-Brown et al., 2009; Hellén et al., 2018). Sesquiterpenes 50 are particularly challenging to measure, due to their low vapour pressure, and therefore their ambient levels are most likely underestimated (Pollmann et al., 2005; Duhl et al., 2008; Kim et al., 2009).

All BVOCs are very reactive with both OH and O_3 and, therefore, the existence of a significant pool of unknown and unmeasured BVOCs has important consequences for the quantification of the ozone budget and ambient concentrations, which are crucial to understand the environmental and societal impacts of ozone pollution. The oxidation of BVOCs by ozone is 55 especially important because it forms additional pollutants, such as secondary organic aerosol, and impacts key chemical processes such as the conversion of NO to NO_2 and, therefore, the formation of ozone via R1-R2, as well as the radical budget (Lewis et al., 2000; Glasius and Goldstein, 2016). Missing a large fraction of BVOCs means that all these processes remain potentially underestimated.

One way to address this problem is to expand the number of VOCs that can be measured. This approach has achieved some 60 success, thanks to comprehensive 2-dimensional gas chromatographic techniques (Pankow et al., 2012; Edwards et al., 2013; Glasius and Goldstein, 2016). However, the chemical complexity of the composition of ambient air makes it difficult, if not impossible, to completely quantify the VOC loading of the atmosphere. An alternative approach is to measure an integrated chemical property of all VOCs, such as the chemical lifetime, which includes all the reactions that remove a given species, in 65 this case O_3 (R3-R9). Instruments to measure directly the total ozone reactivity have been demonstrated by Park et al. (2013) and Matsumoto (2014), and used for laboratory studies of gas-phase ozonolysis reactions (Matsumoto, 2016).

This paper presents an instrument designed to measure total ozone reactivity under ambient, environmental chamber and branch enclosure conditions. The Total Ozone Reactivity System (TORS) was developed from the instrument described by Matsumoto (2014) with several modifications, as described below. Section 2 describes the theoretical and operating principles of TORS, while Sect. 3 and Sect. 4 describe the design and the laboratory characterization of the TORS instrument, respectively. In Sect. 5 the TORS instrument is evaluated with three types of experiments, increasingly approaching ambient conditions: laboratory measurements with known BVOC mixtures, laboratory measurements with small plants, and quasi-ambient measurements in a horticultural glasshouse.



2 Ozone Reactivity

2.1 Reactivity measurements

75 The atmospheric lifetime (τ) of a generic species A is defined as the inverse of its total chemical loss rate, i.e. of its chemical reactivity (R):

$$\tau_{(A)} = \frac{1}{R_{(A)}} = \frac{1}{\sum_i k_i [X]_i} \quad (1)$$

where $[X]_i$ is the concentration of a molecule reacting with A and k_i is the corresponding pseudo first-order rate coefficient. The chemical lifetime of a species has long been considered a useful diagnostic parameter, especially to investigate the loss 80 terms of key atmospheric oxidants, such as the OH radical, which are generally less well known than the respective production terms (Bell et al., 2003).

The comparison between the lifetime measured directly and the lifetime calculated from the independent determination of k_i and $[X]_i$ (Eq. 1) allows us to understand whether all the loss terms for a given species have been accounted for. This approach has been used with success to investigate the budget of the OH radical (Kovacs and Brune, 2001; Ingham et al., 2009; Sinha 85 et al., 2010; Whalley et al., 2016; Fuchs et al., 2017; Sanchez et al., 2018) and, more recently, of the NO_3 radical (Sobanski et al., 2016; Liebmann et al., 2018). Measurements of OH reactivity have also helped to discover previously unknown chemistry in terms of recycling and losses of the OH radical (Di Carlo et al., 2004; Lou et al., 2010; Whalley et al., 2011).

The same principle can be used to investigate the chemical loss of ozone. From reactions R1-R11, the rate of production/loss of tropospheric ozone can be calculated as:

$$90 \frac{d[\text{O}_3]}{dt} = -k_{\text{NO}}[\text{NO}] - k_{\text{NO}_2}[\text{NO}_2] - k_{\text{OH}}[\text{OH}] - k_{\text{HO}_2}[\text{HO}_2] - \sum_i k_i [\text{VOC}]_i - \alpha j_{\text{O}_3}[\text{O}_3] + j_{\text{NO}_2}[\text{NO}_2] \quad (2)$$

where α is the fraction of atomic oxygen that does not reform O_3 via reaction with O_2 (R11). Halogens ($\text{X} = \text{Cl}, \text{Br}, \text{I}$) can also react with ozone to form halogen oxides (XO), although this process is likely minor in continental environments far from the main halogen sources (Monks et al., 2015; Simpson et al., 2015). Under the unpolluted conditions of a forested environment (NO = 50 ppt, NO_2 = 500 ppt, OH = 5×10^6 molecule cm^{-3} , HO_2 = 1×10^8 molecule cm^{-3} , Griffith et al. (2013)) the loss 95 of ozone to NO_2 , OH and HO_2 is a factor of 50-100 times slower than the loss of ozone to NO (Table 1). Under more polluted conditions, NO_2 , OH and HO_2 reactions are even less important as ozone sinks compared to NO.

During the night – when photolysis is zero, and the concentrations of OH and HO_2 are typically 2 orders of magnitude lower than during the day – NO is titrated to NO_2 (R5) soon after sunset, leading to the formation of NO_3 radicals (R6). The rate coefficient of $\text{O}_3 + \text{NO}_2$ is small ($k = 3.52 \times 10^{-17} \text{ cm}^3 \text{ molecule}^{-1} \text{ s}^{-1}$, Table 1) compared to the rate coefficients of 100 most monoterpenes and sesquiterpenes with O_3 (since its emissions are light dependent, isoprene is normally not present at night (Guenther et al., 2012)): for example, 1 ppb of NO_2 has the same O_3 reactivity as 2.7 ppb of α -pinene and 6.2 ppb of limonene. This means that NO_2 can be a significant ozone loss during the night only when its concentration is high compared



to the total BVOC loading, which is usually not the case in unpolluted forested environments. Equation 2 can thus be simplified to:

105
$$\frac{d[\text{O}_3]}{dt} = -k_{\text{NO}}[\text{NO}] - k_{\text{NO}_2}[\text{NO}_2] - \sum_i k_i[\text{VOC}]_i - \alpha j_{\text{O}_3}[\text{O}_3] + j_{\text{NO}_2}[\text{NO}_2] \quad (3)$$

where the NO and photolysis terms are significant only during the day and the NO_2 term is significant only during the night (and under relatively high NO_x conditions). The concentrations of O_3 , NO and NO_2 , their rate coefficients with O_3 and the photolysis rates of O_3 and NO_2 can be measured and/or are well known. Therefore, Eq. 3 can be used to evaluate the contribution of the volatile organic compounds ($\sum_i k_i[\text{VOC}]_i$). As mentioned in Sect. 1, only a handful of the VOCs that react with ozone are routinely measured, which likely leads to underestimation of the VOC contribution to ozone loss. If the loss rate of ozone can be directly measured, it is possible to determine the total VOC loading and compare it with the measured VOCs, thus allowing an estimate of the missing (i.e., non measured) VOCs.

2.2 TORS concept

115 The Total Ozone Reactivity System (TORS) is based on the technique developed by Matsumoto (2014). At its core, the system is a dark flow tube reactor in which a known amount of ozone is reacted with a sample (e.g., NO, unsaturated VOCs). If the change in the concentration of the co-reactants in the sample is small, the reaction follows pseudo first-order kinetics and the change in ozone concentration is described by:

$$[\text{O}_3]_t = [\text{O}_3]_0 \times e^{-k't} \quad (4)$$

120 where $[\text{O}_3]_0$ and $[\text{O}_3]_t$ are, respectively, the initial and final ozone concentrations, k' is the pseudo first-order rate coefficient and t is the reaction time, which corresponds to the reactor residence time and can be determined experimentally (Sect. 4.1). Equation 4 can be solved analytically provided the reaction time and the initial and final O_3 concentrations are known:

$$k' = \frac{-\ln([\text{O}_3]_t/[\text{O}_3]_0)}{t} \quad (5)$$

125 TORS provides a direct measurement of k' , which includes the chemical reactions inside the reactor (described by Eq. 3) plus any other O_3 removal processes, such as the loss of ozone on the reactor wall. Since the reactor is completely dark, the photolysis terms in Eq. 3 can be neglected and the only contributors to the O_3 chemical loss are NO and VOCs. The focus of this study is on the reactivity of VOCs (Sect. 1), and therefore the loss of O_3 due to NO and to the reactor wall need to be subtracted. For the purpose of this work, we define ozone reactivity (R_{O_3}) as:

$$R_{\text{O}_3} = k' - R_{\text{NO}} - R_{\text{wall}} = k' - k_{\text{NO}}[\text{NO}] - R_{\text{wall}} = \sum_i k_i[\text{VOC}]_i \quad (6)$$



where R_{NO} is the removal of O_3 by reaction with NO and R_{wall} is the loss of O_3 on the reactor wall. R_{wall} is a potentially significant parameter in the TORS technique and requires accurate and precise determination (Sect. 4.2). Another potentially important factor is the effect of secondary reactions, which can increase the loss of ozone (R5-R8) causing overestimation of R_{O_3} or can decrease the concentration of VOCs in the sample via reactions other than ozonolysis (e.g., if there is significant formation of NO_3 in the reactor via R6) causing underestimation of R_{O_3} .

Particularly important can be the formation of OH radicals from VOC ozonolysis (Paulson et al., 1999; Rickard et al., 1999; Johnson and Marston, 2008; Alam et al., 2011): to remove this interference an OH scrubber, such as cyclohexane, can be added to the system. Cyclohexane does not react with O_3 , but reacts quickly with OH ($k = 6.97 \times 10^{-12} \text{ cm}^3 \text{ molecule}^{-1} \text{ s}^{-1}$) and forms organic peroxy radicals which combine with HO_2 to form products that do not react with O_3 (Alam et al., 2011). Therefore, cyclohexane acts as an efficient OH scrubber when present at high mixing ratios (ppm level). The effects of ozone loss on the reactor wall and of secondary chemistry of ozonolysis products were investigated with a box-model simulation of the TORS chemistry (Sect. 2.3) and with laboratory characterization experiments (Sect. 4.2).

2.3 Simulation of TORS chemistry

A box-model was used to simulate the chemical reactions occurring in the reactor. The main objective of the model was to assess the effect of the OH radicals generated by the ozonolysis of VOCs and the role of an OH scrubber, as well as the impact of potential interfering chemistry such as removal of ozone by OH, HO_2 and NO_2 (R6-R8), and removal of VOCs by OH and NO_3 .

The model was assembled using the AtChem2 modelling toolkit (Sommariva et al., 2019) with the inorganic chemistry and the oxidation mechanisms of α -pinene and cyclohexane from the Master Chemical Mechanism (MCM v3.3.1, Saunders et al. (2003)). The cyclohexane mechanism was updated to include a more accurate representation of the ring-opening path of the cyclohexoxy radical, following Alam et al. (2011), although the model results were not substantially different from those of a model using the MCM standard cyclohexoxy radical scheme. It must be noted that the model results depend on the VOC used, as the OH yield from ozone + alkene reactions can vary from 0.16 for ethene to 0.90 for 2,3-dimethyl-2-butene (Johnson and Marston, 2008). The choice of α -pinene for the model, as well as for the laboratory experiments (Sect. 5.1) is due to the fact that α -pinene is one of the most abundant BVOC (Guenther et al., 2012). It also has a high OH yield (0.8, Johnson and Marston (2008)), allowing an estimate of the upper bounds of the the potential interferences caused by OH chemistry.

The model was initialized with a range of α -pinene mixing ratios (0.1-50 ppb) and, for each of them, it was run with a range of cyclohexane mixing ratios (0-20 ppm). The initial mixing ratios of NO and NO_2 were 50 and 500 ppt, respectively, representative of an unpolluted forested environment which would be the typical location for TORS measurements (Griffith et al., 2013). The initial O_3 mixing ratio was set to 120 ppb, as used during the experimental work (Sect. 4.3). The model runtime was 300 seconds, covering the range of potential instrument residence times (Sect. 4.1). A summary of the model results is shown in Fig. 1.

The removal of α -pinene during the residence time in the reactor was 3-5% and \sim 7% for initial α -pinene mixing ratios of \geq 0.5 ppb and 0.1 ppb, respectively (Fig. 1a). In the absence of cyclohexane, the removal of α -pinene was slightly higher



(1-2 percentage points) due to reaction with OH radicals. These numbers indicate that the consumption of α -pinene inside the reactor was over an order of magnitude smaller than its initial concentration and, therefore, the chemical system approached 165 the pseudo first-order conditions required for the TORS method to work (Sect. 2.2). The error in the determination of ozone reactivity caused by the assumption of pseudo first-order conditions can be estimated at <4% for α -pinene mixing ratios >10 ppb. As expected (Alam et al., 2011), the reactions with oxidation products of cyclohexane were not significant sinks for ozone: apart from the wall loss, which is not included in the model, the loss of O_3 inside the reactor was less than 1.5% for α -pinene mixing ratios of up to 50 ppb and independent on the concentration of cyclohexane (Fig. 1b).

170 The model results also indicate that the formation of OH radicals from the ozonolysis of α -pinene was partially offset by their destruction via reaction with α -pinene itself and with its reaction products. Fig. 1c shows the difference between the initial and the final concentrations of the OH radical, as calculated by the model. In the absence of cyclohexane, the model calculated net OH production (up to 3×10^5 molecule cm^{-3}) for α -pinene mixing ratios of <1 ppb and net OH destruction (up to 1.3×10^5 molecule cm^{-3}) for α -pinene mixing ratios of 5 ppb or more (Fig. 1c). Compared to the case with zero 175 cyclohexane, the concentration of OH in the reactor decreased by 2 orders of magnitude at levels of cyclohexane between 1 and 5 ppm, depending on the α -pinene level: increasing the cyclohexane mixing ratio above 5 ppm did not cause further decrease in the calculated concentration of OH, nor a reduction in the loss of ozone and α -pinene (Fig. 1a-c).

180 Figure 1d shows that the ozone reactivities determined with 1 and 20 ppm of cyclohexane were essentially the same for α -pinene initial mixing ratios up to 50 ppb. Moreover, the model results show that the differences between the ozone reactivity calculated with and without cyclohexane were between +1% and -5%, depending on the α -pinene level (Fig. 1d). This demonstrates that OH chemistry has a small overall impact on the determination of total ozone reactivity, a conclusion that is supported by the laboratory experiments (Sect. 5.1). Model calculated HO_2 concentrations were less than 1×10^8 molecule cm^{-3} , meaning that ozone reactivity with HO_2 was two orders of magnitude lower than ozone reactivity with α -pinene (at 10 ppb of α -pinene). Only at very low concentrations of α -pinene (<0.1 ppb), HO_2 was a significant sink for ozone.

185 The presence of NO_3 radicals in the reactor is a potentially important interference for the TORS technique, both because its formation consumes O_3 (R6) and because NO_3 reacts quickly with α -pinene ($k = 6.2 \times 10^{-12} cm^3 molecule^{-1} s^{-1}$). Ambient NO_3 is likely lost in the inlet before the reactor, since the transmission of NO_3 through the inlet – a 6 mm diameter, 5 m long teflon tube with a residence time of ~4 seconds – is poor (Dubé et al., 2006). However, NO_3 can be formed inside the reactor via R6 and the model calculated NO_3 formation of the order of 10^6 molecule cm^{-3} for α -pinene mixing ratios >5 ppb. 190 Although the rate coefficient of α -pinene + NO_3 is 5 orders of magnitude larger than the rate coefficient of α -pinene + O_3 , the ozone concentration in the reactor is 6-7 orders of magnitude higher than the concentration of NO_3 . Therefore the reactivity of α -pinene with O_3 was 1-2 orders of magnitude larger than its reactivity with NO_3 (Table 1). It must also be noted that NO_3 formation is only an issue for ambient measurements, not for laboratory, enclosure and environmental chamber experiments under low or zero NO_x conditions.

195 To summarize, the model of the TORS reactor suggest that, under typical operating conditions, the concentrations of HO_2 and NO_3 are too small to compete with BVOCs for reaction with O_3 . Additionally, the model provides no indication that the products of the oxidation of cyclohexane, when used as OH scrubber, can significantly affect the determination of total ozone



reactivity. While ppm levels of cyclohexane effectively eliminate the OH radicals formed by BVOC ozonolysis reactions, the model suggests that ozone reactivities determined with and without an OH scrubber differ by <5%. The model results are in
200 agreement with the discussion in Sect. 2.3, where it was concluded that the decay of O₃ in the TORS reactor is predominantly due to the reactions with NO and VOCs, and potentially to loss on the reactor wall (Eq. 6). It is important to note, however, that the conclusions of the model simulations may vary depending on the chemical conditions in the reactor. Several factors affect the chemistry inside the TORS reactors: the type and mixture of VOCs in the sample, their OH yields, the ambient concentrations of NO and NO₂ and, to a lesser extent, ambient temperature and pressure.

205 3 Instrumentation

3.1 Description of TORS

The operating principles of TORS are described in Sect. 2.2 and a diagram of the TORS instrument is shown in Fig. 2. The reactor is a 1 m long polytetrafluoroethylene (PTFE) tube with an external diameter of 90 mm and an internal diameter of 87.33 mm. Several different materials and geometries for the reactor were tested during the instrument development phase
210 (Sect. 4.2) and this design was found to allow a residence time inside the reactor long enough for the ozonolysis reactions to take place to a suitably measurable extent, while minimizing the consumption of VOCs – in order to maintain pseudo-first order conditions – and the loss of ozone on the reactor wall (Sect. 4.1).

An ozone flow is generated by irradiating a flow of zero air with a UV mercury lamp (UVP Ltd., UK). The ozone flow is mixed with the sample flow just before the reactor and the initial ozone concentration ([O₃]₀) is measured at this point, while
215 the final ozone concentration ([O₃]_t) is measured at the exit point of the reactor (Fig. 2). Depending on the instrument settings, this setup produces an O₃ mixing ratio in the reactor of 100-140 ppb. Ozone concentrations are measured using two identical UV photometric O₃ monitors (Model 49i, Thermo Fisher Scientific, USA). The Model 49i O₃ monitor has a stated detection limit of 1 ppb and a precision of 0.25 ppb at 1 minute averaging time. The reactor can be bypassed using two 3-way teflon valves, so that the two ozone monitors can simultaneously measure the O₃ concentration before it enters the the reactor, thus
220 allowing the ozone measurements to be corrected for any difference between the two monitors (Sect. 4.3). In addition, a T/RH probe (HMP110, Vaisala Oyj, Finland) is inserted in the reactor to monitor temperature and relative humidity. All the flows in the TORS instrument are controlled with mass flow controllers (Brooks Instrument LLC, USA) using a custom-built control box (IGI Systems Ltd, UK). The signals from the ozone monitors, the T/RH probe and the mass flow controllers are logged on a laptop and processed with ad-hoc software in the R programming language.

225 A potentially important factor for TORS is the stability of the ozone source: highly variable levels of O₃ in the ozone flow (Fig. 2) can affect the determination of the ozone reactivity and increase the signal-to-noise ratio of the instrument. The ozone mixing ratio generated by the mercury lamp was found to vary, on average, by 0.4-0.6 ppb (5 minutes, 2- σ), i.e. less than 1%. The ozone reactivity measurements reported in this paper (Sect. 5) were all averaged to 5 minutes.



3.2 Supporting VOC measurements

230 A proton-transfer-reaction time-of-flight mass spectrometer (PTR-QiTof-MS, Ionicon Analytik GmbH, Austria) was used to measure VOC concentrations during the laboratory experiments (Sect. 5.1, Sect. 5.2). The instrument (Sulzer et al., 2014) was operated according to standard operating conditions recommended by the manufacturer (drift pressure = 3.8 mbar, drift tube temperature = 80 °C and E/N = 129 Td), using H_3O^+ as the reagent ion. Calibration was performed using a TO-14A aromatics standard mixture (Airgas Inc., USA). This mixture does not contain biogenic compounds, so a mass transmission curve was
235 used for quantification. Recent work has shown that this approach can be used to quantify uncalibrated species for PTR-MS instruments operating within standard conditions (Holzinger et al., 2019).

240 Measurements of BVOCs can be problematic for monoterpenes and sesquiterpenes, as the PTR technique cannot distinguish between isomers (de Gouw and Warneke, 2007). Typically, when measured by PTR-MS the main fragment ions for monoterpenes and sesquiterpenes are at m/z 81.07 and 149.1, respectively, and this fragmentation is independent of the structure of the isomers (Tani et al., 2003; Kim et al., 2009). Therefore total monoterpene and sesquiterpene concentrations were estimated using the abundances of the protonated parent ions (m/z 137 and 205, respectively) and of the main fragment ions (m/z 81 and 149, respectively). Other compounds associated with biogenic emissions (e.g., substituted monoterpene alcohols, after loss of a neutral H_2O) can also be detected at these fragment ions (Kim et al., 2010) and thus the estimated concentrations shown here may be considered upper limits.

245 The PTR-MS instrument was not available for the experiments outside the laboratory (Sect. 5.3). Instead, samples were taken with adsorption tubes, which were desorbed using a TD Unity-2 thermal desorption unit (Markes Int., UK) and subsequently analysed with a gas chromatograph (GC 7890B, Agilent Technologies, USA) interfaced with a BenchTOF-Select time-of-flight mass spectrometer with tandem ionisation (Markes Int., UK). Further information on the analytical technique and the GC protocol can be found in Alam et al. (2016). The GC-MS analysis were only qualitative due to unavailability of appropriate
250 calibration standards, with the data used to identify the VOCs in the samples.

4 Characterization of TORS

4.1 Residence time

Residence time is one of the key parameters in Eq. 5 and therefore needs to be determined as accurately as possible. The geometry of the reactor and the total flow (sample + ozone) determine the residence time. Three methods were used to determine
255 the residence time: 1) direct measurement using a double injection of acetone 2) indirect measurement via determination of NO reactivity with O_3 and 3) calculation using the flow rate and the internal volume of reactor (5990 cm^3).

Method 1 is illustrated in Fig. 3: the reactor was connected to the PTR-MS and aliquots of 0.05 μl of acetone, in a flow of zero air, were injected simultaneously at the entrance and at the exit of the reactor. Acetone was used as a tracer for these experiments because it is easy to detect with the PTR-MS at m/z 59. The simplest way to determine the residence time is to
260 measure the time lag between the detection of the first and the second acetone peak signals by the PTR-MS (“maxima” in



Fig. 3). However, it must be observed that the flow dynamics inside the reactor are complex and, as a consequence, there is no single value of residence time, but a distribution (Cazorla and Brune, 2010; Huang, 2016). The acetone signal from each injection can also be used to determine the mean residence time in the reactor (“means” in Fig. 3): the results differ from the residence times estimated using the “maxima” calculations by about 30%.

265 Method 2 uses the TORS technique to measure the reactivity of O_3 with NO: since the rate coefficient of $NO + O_3$ is well known ($1.73 \times 10^{-14} \text{ cm}^3 \text{ molecule}^{-1} \text{ s}^{-1}$ at 298 K, with an uncertainty of 17% (Atkinson et al., 2004)), the only unknown variable in Eq. 3 is the reaction time t , in an NO/O_3 only reaction system under pseudo first-order conditions. The average of several experiments conducted at different flow rates is shown in Fig. 4a. Method 3 assumes perfect instant mixing and plug flow in the reactor: the calculation for a range of flow rates is shown in Fig. 4b.

270 All three methods offer internally consistent results, within the respective uncertainties (Fig. 4b). Method 3 agrees well with the acetone injection “means” calculation, but overestimates the residence times determined with method 2 by $\sim 13\%$. Method 2 is the preferred one, because it relies on well known kinetic parameters and it implicitly takes into account the real distribution of flow paths through the reactor. Method 2 also provides a simple test of the TORS functionality using NO instead of a BVOC. In the experiments described in Sect. 5, we used the residence time determined with method 2 with a reactor flow
275 of 2470 sccm (Sect. 4.3).

4.2 Ozone wall loss

One of the most important parameters and key uncertainties of the TORS technique is the ozone wall loss (R_{wall}), as discussed in Sect. 2.2. Other species can be lost on the reactor surface, but these are likely to have little or no impact on the determination of ozone reactivity either because they do not react with O_3 (e.g., multifunctional products of VOC oxidation) or because they
280 are present in too small concentrations.

Measured R_{O_3} is obtained by subtracting the loss of O_3 on the reactor wall (R_{wall}) and, if present, to NO (R_{NO}) from the total loss rate of O_3 (Eq. 6). Small changes in the wall loss could lead to significant variation in the final determination of ozone reactivity. It is therefore important to minimize this parameter in order to reduce the uncertainty of the measurement. In the design stage, several materials and sizes were tested under dry and humid conditions: 1) a glass cylinder (5 x 70 cm), 2) a
285 quartz cylinder (9 x 100 cm), 3) a PFA coil (1.9 x 1524 cm), 4) a PTFE cylinder (9 x 100 cm). Based on these experiments, the large diameter (OD=9 cm, ID = 8.73 cm) PTFE cylinder showed the lowest ozone wall loss and minimal dependence on humidity.

The ozone wall loss was regularly determined during measurements by switching to a flow of zero air instead of the regular sample with a 3-way teflon valve (Fig. 2): in this operating mode there are no reactants (NO or VOCs) in the reactor and the
290 measured ozone reactivity is equal to R_{wall} . During each experiment and measurement period, multiple determinations of the ozone wall loss were made. Figure 5 shows the average R_{wall} determined during a series of laboratory experiments (Sect. 5.1 and Sect. 5.2), as a function of measured humidity, temperature and time. There was a small but noticeable dependence of R_{wall} on humidity. Ambient humidity is usually higher than the range shown in Fig. 5, but because of the dilution of the sample flow by the dry ozone flow before entering the reactor (Fig. 2), the relative humidity in the reactor is always less than 50%. There



295 was no clear dependence of R_{wall} on temperature, at least in the limited range experienced in the laboratory. The ozone wall loss can be expected to vary with time, as the surface of the reactor is passivated and exposed to ambient air, but there was no obvious temporal trend over the nine month period of these experiments (Fig. 5).

Although there was no observable pattern with respect to the measured parameters, it is apparent that there was significant variability in the ozone wall loss and, therefore, it is necessary to measure R_{wall} often during an experiment and/or ambient 300 measurements. The interquartile range of R_{wall} was $0.5 - 1.3 \times 10^{-4} \text{ s}^{-1}$ (mean = $1.1 \times 10^{-4} \text{ s}^{-1}$), which corresponds to the reactivity of 22-58 ppb of α -pinene (mean = 49 ppb). The range of the measured ozone wall losses suggests that the limit of detection of TORS is of the order of a few tens of ppb of α -pinene or the equivalent concentration, in terms of reactivity, of other BVOCs (Table 1). The limit of detection was quantified with laboratory experiments using known concentrations of α -pinene, as described in Sect. 5.1.

305 4.3 TORS operation

The flows in the TORS instrument are constrained by several competing factors (Fig. 2): first, the total flow (sample + ozone) must be larger than the inlet flows of both O_3 monitors, which are fixed at $\sim 1.4 \text{ slpm}$ each. Second, the residence time in the reactor must be long enough to allow the ozonolysis reactions to take place to a measurable extent, but short enough that the consumption of the reactants does not become significant, so that pseudo first-order conditions are maintained (Sect. 2.2).

310 During the design phase of the TORS instrument several combinations of flow settings were experimented with, eventually settling on a sample flow of $\sim 2.3 \text{ slpm}$ and an ozone flow – composed of a flow of zero air through the ozone lamp, plus a dilution flow to control the concentration of ozone and a flow of cyclohexane as OH scrubber – of $\sim 1.5 \text{ slpm}$ (Fig. 2). These settings result in a reactor flow rate of 2470 sccm, corresponding to a residence time of 128 seconds (Sect. 4.1). Since the sample flow is mixed with the ozone flow (Fig. 2), a correction factor needs to be applied to account for the dilution of the 315 sample by the ozone flow. In the experiments and the measurements described in Sect. 5, the mixing ratio of ozone at the entrance of the reactor was $\sim 120 \text{ ppb}$. The instrument settings, such as the residence time and the ozone concentration, can in principle be varied to adjust the sensitivity of TORS for environments with different values of R_{O_3} .

Once the flows are set, the basic operation cycle of the TORS instrument consists of 3 main steps:

1. “bypass mode” to check the agreement between the two O_3 monitors: the sample flow is substituted with an equal flow 320 of zero air and the reactor is bypassed for a period of approximately 15 minutes. In this mode, both monitors measure the O_3 concentration in zero air (i.e., with no reactants) before the entrance of the reactor, so that a correction factor can be derived if they differ. In this work, the difference between the O_3 monitors was checked at the start and at the end of each experiment/measurement period, every day, and was typically $\sim 1 \text{ ppb}$.
2. “wall loss mode” to determine R_{wall} (Eq. 6): the sample flow is substituted with an equal flow of zero air inside the 325 reactor for a period of approximately half an hour. The effect of the humidity change in the reactor within such a short period of time was found to be negligible. In this work, the wall loss was determined every 2-3 hours.
3. “sampling mode”, the main operation mode of the instrument with the sample flow containing BVOCs.



This procedure was followed during all the experiments and measurements described in Sect. 5.

5 Evaluation of TORS

330 The TORS instrument was tested in a series of experiments to evaluate its functionality and potential. The experiments were designed and conducted in order of increasing complexity from individual species in laboratory conditions to the complex BVOCs mixture of a horticultural glasshouse. The TORS instrument was at first tested in the laboratory using pure α -pinene (Sect. 5.1), followed by emissions from small plants (Sect. 5.2). After these tests showed that the instrument was behaving as expected under controlled conditions, it was deployed in a glasshouse containing various aromatic plants to demonstrate that
335 TORS can measure total ozone reactivity under quasi-ambient conditions (Sect. 5.3).

340 It must be noted that the rate coefficients of O_3 with BVOCs span several orders of magnitude (Table 1). Therefore, for individual species in isolation, a measured ozone reactivity of (for example) $2.36 \times 10^{-5} \text{ s}^{-1}$ corresponds equally to 1.9 ppm of camphene, 10 ppb of α -pinene, 74 ppb of isoprene, 80 ppt of β -caryophyllene. This affects the interpretation of R_{O_3} measurements by TORS, particularly if the composition of the sample is not known, as would be the case when taking ambient measurements.

5.1 Laboratory experiments

Several laboratory experiments were carried out using known concentrations of a selected biogenic compound. A thermostated diffusion tube and pure α -pinene (98%, from Sigma-Aldrich) in zero air were used to provide a constant source of BVOC. The diffusion rate was controlled by varying the temperature of the diffusion tube and determined by regularly weighing it with a
345 precision balance over a period of several weeks. The concentration of α -pinene was then calculated from the diffusion rate and confirmed with direct measurements by PTR-MS (Sect. 3.2).

The values of R_{O_3} measured during several experiments were compared with the values calculated using the known concentrations of α -pinene in the sample (Eq. 6). The data show reasonable agreement – within the combined uncertainties of the instrument and of the α -pinene + O_3 rate coefficient (41%, Atkinson et al. (2004)) – between the calculated and measured
350 reactivity for α -pinene mixing ratios larger than 40 ppb (Fig. 6a). At mixing ratios below 10 ppb of α -pinene, the measured reactivities cannot be statistically distinguished from each other and from zero. Measured R_{O_3} corresponding to concentrations of α -pinene $> 14 \text{ ppb}$ are linearly correlated ($r^2 = 0.993$) with a slope of $1.33 \times 10^{-6} \pm 1.12 \times 10^{-7} \text{ s}^{-1}/\text{ppb}$, corresponding to the sensitivity of the instrument, and an intercept of $7 \times 10^{-5} \pm 9 \times 10^{-6} \text{ s}^{-1}$ (Fig. 6a).

Based on these experiments, the TORS detection limit, for a residence time of 128 seconds, can be estimated between
355 4.5×10^{-5} and $9.0 \times 10^{-5} \text{ s}^{-1}$, corresponding to ozone reactivities equivalent to 20-40 ppb of α -pinene (Table 1). These values are consistent with the estimates based on the range of measured R_{wall} , as discussed in Sect. 4.2; the actual detection limit for a given set of measurements depends on the magnitude of the ozone wall loss, which can vary significantly (Fig. 5). These values are comparable to the detection limit of the instrument described by (Matsumoto, 2014) of $1.4 \times 10^{-4} \text{ s}^{-1}$, for a residence time of 57 seconds.



360 Some experiments were conducted without adding cyclohexane to the ozone flow (Fig. 2) to verify the effect of the OH
scrubber, as discussed in Sect. 2.3. Ozonolysis of BVOCs is known to generate OH radicals with different yields (Rickard
et al., 1999; Johnson and Marston, 2008) which may lead to consumption of BVOCs by OH in the reactor, thus causing
underestimation of R_{O_3} . However, the experiments where the OH scrubber was used did not show substantially different
365 results from those where it was not used (Fig. 6b). Measured R_{O_3} with ~ 30 ppb of α -pinene was $6.75 \times 10^{-5} \pm 2.41 \times 10^{-5}$
 s^{-1} with cyclohexane and $6.33 \times 10^{-5} \pm 2.12 \times 10^{-5} s^{-1}$ without cyclohexane: the corresponding p-value was 0.39, indicating
that the difference between the two measurements is not statistically significant. The difference between the ozone reactivities
determined with and without OH scrubber was $\sim 6\%$, in agreement with the modelling results, which showed that the presence
of the OH scrubber affects the measurements of total ozone reactivity by 5% or less (Sect. 2.3). While this is less than the
precision of the ozone monitors (Sect. 3.1) we note that, in principle, the comparison of total ozone reactivity measurements
370 with and without an OH scrubber can yield additional information on the speciation of the VOC mixture in the sample.

5.2 Plant experiments

375 Laboratory experiments were carried out using small aromatic plants in a controlled environment to test the TORS instrument
under more realistic conditions. Three plants of lemongrass (*Thymus citriodorus*) were enclosed in a Teflon bag – with an
approximate volume of 0.1 m^3 – filled with a continuous flow of zero air. A halogen lamp was located over the bag and a
temperature/humidity probe (Vaisala HMP110) was inserted into the bag, together with a small fan to ensure homogeneous
conditions. The natural humidity of the plants caused the humidity in the bag to rise over the course of the experiment, but
relative humidity remained below 50% inside the TORS reactor due to dilution with the dry ozone flow (Fig. 2) and therefore
did not affect the loss of O_3 on the reactor wall, as discussed in Sect. 4.2. The PTR-MS was connected to the bag to identify
380 and quantify the BVOCs that constitute the plant emissions (Sect. 3.2). The TORS instrument and the PTR-MS sampled
continuously from the Teflon bag during the experiment, which had a duration of about 48 hours.

Figure 7 shows the ozone reactivity measurements of the lemongrass experiment, together with the reactivity calculated
using the BVOCs measurements by PTR-MS. The interquartile range of measured R_{O_3} was $3 - 11 \times 10^{-5} s^{-1}$ for the first
experiment and $7 - 10 \times 10^{-5} s^{-1}$ for the second experiment, with mean values of 7×10^{-5} and $9 \times 10^{-5} s^{-1}$, respectively.

385 Measured ozone reactivity increased by about a factor of 2 when the lamp was turned on, due to increased emissions of all
BVOCs and, in particular, of the more reactive ones (i.e., monoterpenes and sesquiterpenes, Table 1). This is because when the
lamp was switched on the temperature inside the bag increased (by $\sim 10^\circ\text{C}$, Fig. 7), as well as the light. Isoprene emissions are
controlled by both light and temperature, but monoterpenes and sesquiterpenes emissions are mostly controlled by temperature
and have an exponential response to temperature (Duhl et al., 2008; Guenther et al., 2012; Hellén et al., 2018). Therefore, the
emissions of these more reactive compounds tend to increase faster than those of isoprene when temperature rises quickly.

390 To calculate R_{O_3} from the PTR-MS measurements (Sect. 3.2) using Eq. 6, a number of assumptions have to be made. The
only BVOC that the Proton Transfer Reaction technique can uniquely identify is isoprene. All monoterpenes and sesquiterpenes
have the same molecular weight (136.24 and 204.36 g/mol, respectively) and therefore are very difficult to distinguish from
each other using a soft ionization technique (de Gouw and Warneke, 2007). The PTR-MS instrument effectively reports the



sum of monoterpenes and the sum of sesquiterpenes. To account for this problem, estimated low and high R_{O_3} limits were
395 calculated. Lemonthyme is an evergreen broadleaf plant, whose main emissions (besides isoprene) are α -pinene, β -pinene,
 β -ocimene (monoterpenes) and β -caryophyllene, α -farnesene (sesquiterpenes) (Fares et al., 2011; Guenther et al., 2012). The
lower limit R_{O_3} estimate was calculated assuming that the measured monoterpene signal was solely due to β -pinene and that
the measured sesquiterpene signal was solely due to α -farnesene. The higher limit R_{O_3} estimate was calculated assuming that
400 the measured monoterpene signal was solely due to β -ocimene and that the measured sesquiterpene signal was solely due to
 β -caryophyllene. This provides a range of R_{O_3} which likely includes that of the particular BVOCs mixture emitted by the
lemonthyme plants (Table 1). The calculated low and high R_{O_3} limit estimates are compared to the TORS measurements in
Fig. 7. The TORS measured reactivities were within the range of these estimates and followed the same pattern, with higher
values when the light was on and the temperature higher.

5.3 Glasshouse experiments

405 In order to evaluate the TORS technique under quasi-ambient conditions, the instrument was deployed in a horticultural
glasshouse containing a range of aromatic plants. The glasshouse is a similar environment to ambient and was subject to a
continuous inflow of ambient air, but, being a semi-enclosed system, the concentrations of BVOCs emitted from the plants are
higher and the concentrations of NO lower than the external environment, resulting in a stronger R_{O_3} signal. The glasshouse
is located at the Winterbourne House and Garden (<https://www.winterbourne.org.uk/>), adjacent to the University of Birming-
410 ham campus, and has an approximate volume of 200 m³. The following plants were inside the glasshouse during the sampling
period: Fringed “French” Lavender (*Lavandula dentata* var. *candicans*), Lemon Verbena (*Aloysia triphylla*), Scented Leaf Ger-
anium (*Pelargonium* “Prince of Orange”, *Pelargonium* “Radula”) and several varieties of Citrus (*Citrus x limon*, *Citrus* “Tahiti”,
Citrus reticulata “Clementine”).

415 The TORS instrument was setup in a similar way as in the plant experiments (Sect. 5.2), with regular determination of the
ozone wall loss using a flow of zero air instead of the ambient flow. The measurements were taken over a period of two weeks
in early June 2018; during this period the weather was dry (mean RH = 57%) with temperatures reaching a maximum of 39 °C
inside the glasshouse (mean = 15 °C). Cyclohexane was used as OH scrubber only during the second week of measurements.
The PTR-MS was not available at the glasshouse, but two air samples were taken on two different days using adsorption tubes
420 and qualitatively analyzed by GC-MS (Sect. 3.2). The GC data were used to determine the most important monoterpenes and
sesquiterpenes in the air inside the glasshouse, based on their relative abundance.

The ozone reactivity measurements made in the glasshouse are shown in Fig. 8. For the period without cyclohexane the
interquartile range was $2.11 - 5.01 \times 10^{-4} \text{ s}^{-1}$ with a mean of $3.63 \times 10^{-4} \text{ s}^{-1}$. For the period with cyclohexane the interquartile
range was $2.01 - 4.09 \times 10^{-4} \text{ s}^{-1}$ with a mean of $3.07 \times 10^{-4} \text{ s}^{-1}$. Taking into account the natural variability of plant emissions,
these numbers suggest that the use of an OH scrubber does not change significantly the TORS measurements, in keeping with
425 the laboratory experiments (Sect. 5.1) and the model results of the chemistry inside the reactor (Sect. 2.3).

In the absence of BVOC measurements, an estimate of the ozone reactivity was calculated using the qualitative informa-
tion obtained from the GC-MS analysis of the adsorption tubes and emission factors from Guenther et al. (2012): broadleaf



evergreen plants emit isoprene, monoterpenes and sesquiterpenes in a proportion of approximately 1:0.1:0.02. However, Fares et al. (2011) found that Citrus plants, several types of which were present on the glasshouse, emit more monoterpenes than isoprene. Since most monoterpenes are more reactive with ozone than isoprene (Table 1), the estimates of R_{O_3} discussed below are relatively insensitive to the actual isoprene concentration.

Analysis of the adsorption tubes showed that the most important monoterpenes were limonene, β -pinene, camphene, myrcene and the most important sesquiterpenes were longifolene and farnesene. Based on these results, a high R_{O_3} was estimated assuming 100 ppb of isoprene, 25 ppb of myrcene and 5 ppb of α -farnesene. A low R_{O_3} was estimated assuming 50 ppb of isoprene, 5 ppb of camphene and 1 ppb of longifolene. The estimated low and high R_{O_3} are of the same magnitude as the TORS measurements (Fig. 8).

In contrast to the laboratory experiments, which were performed using zero air (Sect. 5.1 and Sect. 5.2), the ozone reactivity measurements in the glasshouse were affected by ambient NO (R5). Measurements of NO were not available in the glasshouse, but ambient data from a nearby site can be used to estimate the role of NO. These observations were taken at the Automatic Urban and Rural Network monitoring site of Birmingham Acocks Green, which is located \sim 7 km from Winterbourne House and is considered a urban background site (https://uk-air.defra.gov.uk/networks/site-info?site_id=AGRN). The mean NO mixing ratio reported at the Acocks Green site during the measurement period was 2 ppb (interquartile range = 1-2.6 ppb).

The average total ozone reactivity showed a clear diel pattern (Fig. 9), with maximum values of about $6 \times 10^{-4} \text{ s}^{-1}$ around 06:00 (approximately one hour after dawn) and was anticorrelated with ambient temperature (Fig. 8). BVOCs emissions are driven by both light and temperature and are therefore higher during the day (Fares et al., 2011; Hellén et al., 2018). Likewise, NO concentrations are higher during day, due to traffic emissions. Therefore, it may be expected that measured R_{O_3} (from both BVOCs and NO) is higher during the daylight hours, which was in fact observed during the laboratory experiments with the lemongrass plants (Fig. 7). However, under ambient conditions, BVOCs react during the day with OH radicals at a faster rate than they react with O_3 (Atkinson et al., 2006; Johnson and Marston, 2008). As a result, ozone reactivity tends peak in the early morning (Fig. 9), when the NO and BVOCs emissions start increasing, but the concentration of OH is still too low to compete with O_3 for BVOC removal (Hellén et al., 2018).

An assessment of the contribution of NO to the total ozone reactivity has to take into account a number of factors. First, it must be considered that, since the $\text{NO} + \text{O}_3$ reaction is very fast (Table 1), a fraction of ambient NO is removed by ambient ozone before it enters the TORS reactor. The inlet residence time is \sim 4 seconds and the lifetime of NO with 20-30 ppb of O_3 (typical ambient levels) is 3-5 seconds, which means that the concentration of NO drops to \sim 36% of the ambient concentration while inside the inlet line (Fig. 2). Additionally, it may be assumed that the concentration of NO inside the glasshouse was lower than outside, especially considering that the glasshouse is located 50 m or more from nearby roads. Therefore, under the assumption that the concentration of NO in the reactor is \sim 20% of the ambient concentration, R_{NO} can be subtracted from the total O_3 reactivity and R_{O_3} can be derived from Eq. 6. Based on these approximations, the ozone reactivity due to BVOCs in the glasshouse can be estimated at $2-5 \times 10^{-4} \text{ s}^{-1}$, on average. Figure 9 shows that NO reactivity dominates during the day, but is not significant during the night when BVOCs control ozone loss. Caution should be exercised in interpreting



these measurements and results, as the assumption about NO levels in the glasshouse could not be verified at the time of the measurements.

6 Summary and Future Work

465 An instrument to measure total ozone reactivity, named Total Ozone Reactivity System (TORS), was developed, characterized and tested under controlled conditions in the laboratory; both individual compounds and small plants were used. The instrument was deployed inside a horticultural glasshouse containing a range of aromatic plants to evaluate its functionality under quasi-ambient conditions.

470 The TORS instrument was able to measure O_3 reactivities with BVOCs (R_{O_3}) of $4.5 - 9.0 \times 10^{-5} \text{ s}^{-1}$ or more, corresponding to 20-40 ppb of α -pinene, 150-300 ppb of isoprene or 160-320 ppt of β -caryophyllene. These mixing ratios are larger than typical ambient levels, but can be found in enclosure studies (Duhl et al., 2008; Bouvier-Brown et al., 2009) and can easily be reproduced in laboratory and environmental chamber experiments. An OH scrubber (cyclohexane) was used to remove the OH radicals formed by the ozonolysis of BVOCs; however, simulations of the chemistry inside the TORS reactor using a Master Chemical Mechanism (MCM v3.3.1) box-model found that the formation of OH from BVOC + O_3 reactions affected 475 the measurements of R_{O_3} by <5%, under the conditions used during the experiments.

480 Further work will improve the stability of the signal, reduce the signal noise and the detection limit. This may require using ozone monitors with higher precision and/or a more stable O_3 generator, as well as a detailed exploration of the various parameters affecting TORS: gas flows, residence time, relative humidity, OH scrubber levels, ozone concentrations. In the future, TORS will be able to make ambient measurements, especially in environments with high BVOC loading, to improve understanding of the role of natural emissions on the ozone budget and the oxidative capacity of the atmosphere.

Competing interests. The authors declare no competing interests.

Acknowledgements. Thanks to D. Blenkhorn, V. Matthaios, K. Vohra, D. Komalasari for their help with some of the experiments and to the University of Birmingham Biosciences Workshop for their continuous assistance. Special thanks to the staff of the Winterbourne House and Garden for their support and to Prof. Jun Matsumoto for his advice and kind hospitality. Funding provided by NERC (NE/P003524/1) and 485 the UoB-Waseda Research Collaboration Fund.



References

Alam, M. S., Camredon, M., Rickard, A. R., Carr, T., Wyche, K. P., Hornsby, K. E., Monks, P. S., and Bloss, W. J.: Total radical yields from tropospheric ethene ozonolysis, *Phys. Chem. Chem. Phys.*, 13, 11 002–11 015, <https://doi.org/10.1039/c0cp02342f>, 2011.

Alam, M. S., Stark, C., and Harrison, R. M.: Using variable ionization energy time-of-flight mass spectrometry with comprehensive GCxGC to identify isomeric species, *Anal. Chem.*, 88, 4211–4220, <https://doi.org/10.1021/acs.analchem.5b03122>, 2016.

Atkinson, R., Baulch, D. L., Cox, R. A., Crowley, J. N., Hampson, R. F., Hynes, R. G., Jenkin, M. E., Rossi, M. J., and Troe, J.: Evaluated kinetic and photochemical data for atmospheric chemistry: Volume I – gas phase reactions of Ox, HOx, NOx and SOx species, *Atmos. Chem. Phys.*, 4, 1461–1738, <https://doi.org/10.5194/acp-4-1461-2004>, <https://www.atmos-chem-phys.net/4/1461/2004/>, 2004.

Atkinson, R., Baulch, D. L., Cox, R. A., Crowley, J. N., Hampson, R. F., Hynes, R. G., Jenkin, M. E., Rossi, M. J., and Troe, J.: Evaluated kinetic and photochemical data for atmospheric chemistry: Volume II – gas phase reactions of organic species, *Atmos. Chem. Phys.*, 6, 3625–4055, <https://doi.org/10.5194/acp-6-3625-2006>, <https://www.atmos-chem-phys.net/6/3625/2006/>, 2006.

Bell, N., Heard, D. E., Pilling, M. J., and Tomlin, A. S.: Atmospheric lifetime as a probe of radical chemistry in the boundary layer, *Atmos. Environ.*, 37, 2193–2205, [https://doi.org/10.1016/S1352-2310\(03\)00157-2](https://doi.org/10.1016/S1352-2310(03)00157-2), 2003.

Bouvier-Brown, N. C., Holzinger, R., Palitzsch, K., and Goldstein, A. H.: Large emissions of sesquiterpenes and methyl chavicol quantified from branch enclosure measurements, *Atmos. Environ.*, 43, 389–401, <https://doi.org/10.1016/j.atmosenv.2008.08.039>, 2009.

Cazorla, M. and Brune, W. H.: Measurement of ozone production sensor, *Atmos. Meas. Tech.*, 3, 545–555, <https://doi.org/10.5194/amt-3-545-2010>, <https://www.atmos-meas-tech.net/3/545/2010/>, 2010.

de Gouw, J. and Warneke, C.: Measurements of volatile organic compounds in the Earth's atmosphere using proton-transfer-reaction mass spectrometry, *Mass Spectrom. Rev.*, 26, 223–257, <https://doi.org/10.1002/mas.20119>, 2007.

Di Carlo, P., Brune, W. H., Martinez, M., Harder, H., Lesher, R., Ren, X., Thornberry, T., Carroll, M. A., Young, V., Shepson, P. B., Riemer, D., Apel, E., and Campbell, C.: Missing OH reactivity in a forest: evidence for unknown reactive biogenic VOCs, *Science*, 304, 722–725, <https://doi.org/10.1126/science.1094392>, 2004.

Dubé, W. P., Brown, S. S., Osthoff, H. D., Nunley, M. R., Ciciora, S. J., Paris, M. W., McLaughlin, R. J., and Ravishankara, A. R.: Aircraft instrument for simultaneous, in situ measurement of NO₃ and N₂O₅ via pulsed cavity ring-down spectroscopy, *Rev. Sci. Instrum.*, 77, 034 101, <https://doi.org/10.1063/1.2176058>, 2006.

Duhl, T. R., Helmig, D., and Guenther, A.: Sesquiterpene emissions from vegetation: a review, *Biogeosciences*, 5, 761–777, <https://doi.org/10.5194/bg-5-761-2008>, <https://www.biogeosciences.net/5/761/2008/>, 2008.

Edwards, S. J., Lewis, A. C., Andrews, S. J., Lidster, R. T., Hamilton, J. F., and Rhodes, C. N.: A compact comprehensive two-dimensional gas chromatography (GCxGC) approach for the analysis of biogenic VOCs, *Anal. Methods*, 5, 141–150, <https://doi.org/10.1039/c2ay25710f>, 2013.

Fares, S., Gentner, D. R., Park, J.-H., Ormeno, E., Karlik, J., and Goldstein, A. H.: Biogenic emissions from citrus species in California, *Atmos. Environ.*, 45, 4557–4568, <https://doi.org/10.1016/j.atmosenv.2011.05.066>, 2011.

Fuchs, H., Novelli, A., Rolletter, M., Hofzumahaus, A., Pfannerstill, E. Y., Kessel, S., Edtbauer, A., Williams, J., Michoud, V., Dusanter, S., Locoge, N., Zannoni, N., Gros, V., Truong, F., Sarda-Esteve, R., Cryer, D. R., Brumby, C. A., Whalley, L. K., Stone, D., Seakins, P. W., Heard, D. E., Schoemaecker, C., Blocquet, M., Coudert, S., Batut, S., Fittschen, C., Thame, A. B., Brune, W. H., Ernest, C., Harder, H., Muller, J. B. A., Elste, T., Kubistin, D., Andres, S., Bohn, B., Hohaus, T., Holland, F., Li, X., Rohrer, F., Kiendler-Scharr, A., Tillmann, R., Wegener, R., Yu, Z., Zou, Q., and Wahner, A.: Comparison of OH reactivity measurements in the atmospheric simulation



chamber SAPHIR, *Atmos. Meas. Tech.*, 10, 4023–4053, <https://doi.org/10.5194/amt-10-4023-2017>, <https://www.atmos-meas-tech.net/10/4023/2017/>, 2017.

525 Glasius, M. and Goldstein, A. H.: Recent discoveries and future challenges in atmospheric organic chemistry, *Environ. Sci. Technol.*, 50, 2754–2764, <https://doi.org/10.1021/acs.est.5b05105>, 2016.

Goldstein, A. H. and Galbally, I. E.: Known and unexplored organic constituents in the Earth's atmosphere, *Environ. Sci. Technol.*, 41, 1514–1521, <https://doi.org/10.1021/es072476p>, 2007.

530 Griffith, S. M., Hansen, R. F., Dusanter, S., Stevens, P. S., Alaghmand, M., Bertman, S. B., Carroll, M. A., Erickson, M., Galloway, M., Grossberg, N., Hottle, J., Hou, J., Jobson, B. T., Kammerath, A., Keutsch, F. N., Lefer, B. L., Mielke, L. H., O'Brien, A., Shepson, P. B., Thurlow, M., Wallace, W., Zhang, N., and Zhou, X. L.: OH and HO₂ radical chemistry during PROPHET 2008 and CABINEX 2009 – Part 1: measurements and model comparison, *Atmos. Chem. Phys.*, 13, 5403–5423, <https://doi.org/10.5194/acp-13-5403-2013>, <https://www.atmos-chem-phys.net/13/5403/2013/>, 2013.

535 Guenther, A. B., Jiang, X., Heald, C. L., Sakulyanontvittaya, T., Duhl, T., Emmons, L. K., and Wang, X.: The Model of Emissions of Gases and Aerosols from Nature version 2.1 (MEGAN2.1): an extended and updated framework for modeling biogenic emissions, *Geosci. Model Dev.*, 5, 1471–1492, <https://doi.org/10.5194/gmd-5-1471-2012>, <https://www.geosci-model-dev.net/5/1471/2012/>, 2012.

Hellén, H., Praplan, A. P., Tykkä, T., Ylivinkka, I., Vakkari, V., Bäck, J., Petäjä, T., Kulmala, M., and Hakola, H.: Long-term measurements of volatile organic compounds highlight the importance of sesquiterpenes for the atmospheric chemistry of a boreal forest, *Atmos. Chem. Phys.*, 18, 13 839–13 863, <https://doi.org/10.5194/acp-18-13839-2018>, <https://www.atmos-chem-phys.net/18/13839/2018/>, 2018.

540 Holzinger, R., Acton, W. J. F., Bloss, W. J., Breitenlechner, M., Crilley, L. R., Dusanter, S., Gonin, M., Gros, V., Keutsch, F. N., Kiendler-Scharr, A., Kramer, L. J., Krechmer, J. E., Languille, B., Locoge, N., Lopez-Hilfiker, F., Materić, D., Moreno, S., Nemitz, E., Quéléver, L. L. J., Sarda Esteve, R., Sauvage, S., Schallhart, S., Sommariva, R., Tillmann, R., Wedel, S., Worton, D. R., Xu, K., and Zaytsev, A.: Validity and limitations of simple reaction kinetics to calculate concentrations of organic compounds from ion counts in PTR-MS, *Atmos. Meas. Tech. Discuss.*, pp. 1–29, <https://doi.org/10.5194/amt-2018-446>, 32, 2019.

545 Huang, H.: Development of an instrument for the in situ measurement of atmospheric ozone production rates, Ph.D. thesis, School of Geography, Earth and Environmental Sciences, University of Birmingham, 2016.

Ingham, T., Goddard, A., Whalley, L. K., Furneaux, K. L., Edwards, P. M., Seal, C. P., Self, D. E., Johnson, G. P., Read, K. A., Lee, J. D., and Heard, D. E.: A flow-tube based laser-induced fluorescence instrument to measure OH reactivity in the troposphere, *Atmos. Meas. Tech.*, 2, 465–477, <https://doi.org/10.5194/amt-2-465-2009>, <https://www.atmos-meas-tech.net/2/465/2009/>, 2009.

550 Johnson, D. and Marston, G.: The gas-phase ozonolysis of unsaturated volatile organic compounds in the troposphere, *Chem. Soc. Rev.*, 37, 699–716, <https://doi.org/10.1039/b704260b>, 2008.

Kim, S., Karl, T., Helming, D., Daly, R., Rasmussen, R., and Guenther, A.: Measurement of atmospheric sesquiterpenes by proton transfer reaction-mass spectrometry (PTR-MS), *Atmos. Meas. Tech.*, 2, 99–112, <https://doi.org/10.5194/amt-2-99-2009>, <https://www.atmos-meas-tech.net/2/99/2009/>, 2009.

555 Kim, S., Karl, T., Guenther, A., Tyndall, G., Orlando, J., Harley, P., Rasmussen, R., and Apel, E.: Emissions and ambient distributions of biogenic volatile organic compounds (BVOC) in a ponderosa pine ecosystem: interpretation of PTR-MS mass spectra, *Atmos. Chem. Phys.*, 10, 1759–1771, <https://doi.org/10.5194/acp-10-1759-2010>, <https://www.atmos-chem-phys.net/10/1759/2010/>, 2010.

Kovacs, T. A. and Brune, W. H.: Total OH loss rate measurement, *J. Atmos. Chem.*, 39, 105–122, <https://doi.org/10.1023/a:1010614113786>, 2001.



560 Lewis, A. C., Carslaw, N., Marriott, P. J., Kinghorn, R. M., Morrison, P., Lee, A. L., Bartle, K. D., and Pilling, M. J.: A larger pool of ozone-forming carbon compounds in urban atmospheres, *Nature*, 405, 778–781, <https://doi.org/10.1038/35015540>, 2000.

565 Liebmann, J. M., Muller, J. B. A., Kubistin, D., Claude, A., Holla, R., Plass-Dülmer, C., Lelieveld, J., and Crowley, J. N.: Direct measurements of NO₃ reactivity in and above the boundary layer of a mountaintop site: identification of reactive trace gases and comparison with OH reactivity, *Atmos. Chem. Phys.*, 18, 12 045–12 059, <https://doi.org/10.5194/acp-18-12045-2018>, <https://www.atmos-chem-phys.net/18/12045/2018/>, 2018.

570 Lou, S., Holland, F., Rohrer, F., Lu, K., Bohn, B., Brauers, T., Chang, C. C., Fuchs, H., Häseler, R., Kita, K., Kondo, Y., Li, X., Shao, M., Zeng, L., Wahner, A., Zhang, Y., Wang, W., and Hofzumahaus, A.: Atmospheric OH reactivities in the Pearl River Delta – China in summer 2006: measurement and model results, *Atmos. Chem. Phys.*, 10, 11 243–11 260, <https://doi.org/10.5194/acp-10-11243-2010>, <https://www.atmos-chem-phys.net/10/11243/2010/>, 2010.

575 570 Matsumoto, J.: Measuring biogenic volatile organic compounds (BVOCs) from vegetation in terms of ozone reactivity, *Aerosol Air Qual. Res.*, 14, 197–206, <https://doi.org/10.4209/aaqr.2012.10.0275>, 2014.

580 Matsumoto, J.: Temperature dependence of rate constant for the gas-phase reaction of ozone with linalool, *Chem. Lett.*, 45, 1102–1104, <https://doi.org/10.1246/cl.160500>, 2016.

585 Monks, P. S., Archibald, A. T., Colette, A., Cooper, O., Coyle, M., Derwent, R., Fowler, D., Granier, C., Law, K. S., Mills, G. E., Stevenson, D. S., Tarasova, O., Thouret, V., von Schneidemesser, E., Sommariva, R., Wild, O., and Williams, M. L.: Tropospheric ozone and its precursors from the urban to the global scale from air quality to short-lived climate forcer, *Atmos. Chem. Phys.*, 15, 8889–8973, <https://doi.org/10.5194/acp-15-8889-2015>, <https://www.atmos-chem-phys.net/15/8889/2015/>, 28, 2015.

590 Pankow, J. F., Luo, W., Melnychenko, A. N., Barsanti, K. C., Isabelle, L. M., Chen, C., Guenther, A. B., and Rosenstiel, T. N.: Volatilizable biogenic organic compounds (VBOCs) with two dimensional gas chromatography-time of flight mass spectrometry (GCxGC-TOFMS): sampling methods, VBOC complexity, and chromatographic retention data, *Atmos. Meas. Tech.*, 5, 345–361, <https://doi.org/10.5194/amt-5-345-2012>, <https://www.atmos-meas-tech.net/5/345/2012/>, 2012.

Park, J., Guenther, A. B., and Helmig, D.: Ozone reactivity of biogenic volatile organic compound (BVOC) emissions during the Southeast Oxidant and Aerosol Study (SOAS), in: AGU 2013 Fall Meeting, 2013.

595 Paulson, S. E., Chung, M. Y., and Hasson, A. S.: OH radical formation from the gas-phase reaction of ozone with terminal alkenes and the relationship between structure and mechanism, *J. Phys. Chem. A*, 103, 8125–8138, <https://doi.org/10.1021/jp991995e>, 1999.

Pollmann, J., Ortega, J., and Helmig, D.: Analysis of atmospheric sesquiterpenes: sampling losses and mitigation of ozone interferences, *Environ. Sci. Technol.*, 39, 9620–9629, <https://doi.org/10.1021/es050440w>, 2005.

Rickard, A. R., Johnson, D., McGill, C. D., and Marston, G.: OH yields in the gas-phase reactions of ozone with alkenes, *J. Phys. Chem. A*, 103, 7656–7664, <https://doi.org/10.1021/jp9916992>, 1999.

595 Sanchez, D., Jeong, D., Seco, R., Wrangham, I., Park, J.-H., Brune, W. H., Koss, A., Gilman, J., de Gouw, J., Misztal, P., Goldstein, A., Baumann, K., Wennberg, P. O., Keutsch, F. N., Guenther, A., and Kim, S.: Intercomparison of OH and OH reactivity measurements in a high isoprene and low NO environment during the Southern Oxidant and Aerosol Study (SOAS), *Atmos. Environ.*, 174, 227–236, <https://doi.org/10.1016/j.atmosenv.2017.10.056>, 2018.

Saunders, S. M., Jenkin, M. E., Derwent, R. G., and Pilling, M. J.: Protocol for the development of the Master Chemical Mechanism, MCM v3 (Part A): tropospheric degradation of non-aromatic volatile organic compounds, *Atmos. Chem. Phys.*, 3, 161–180, <https://doi.org/10.5194/acp-3-161-2003>, <https://www.atmos-chem-phys.net/3/161/2003/>, 2003.



Simpson, W. R., Brown, S. S., Saiz-Lopez, A., Thornton, J. A., and von Glasow, R.: Tropospheric halogen chemistry: sources, cycling, and impacts, *Chem. Rev.*, 115, 4035–4062, <https://doi.org/10.1021/cr5006638>, 2015.

Sinha, V., Williams, J., Lelieveld, J., Ruuskanen, T. M., Kajos, M. K., Patokoski, J., Hellen, H., Hakola, H., Mogensen, D., Boy, M., Rinne, J., and Kulmala, M.: OH reactivity measurements within a boreal forest: evidence for unknown reactive emissions, *Environ. Sci. Technol.*, 44, 6614–6620, <https://doi.org/10.1021/es101780b>, 2010.

Sobanski, N., Tang, M. J., Thieser, J., Schuster, G., Pöhler, D., Fischer, H., Song, W., Sauvage, C., Williams, J., Fachinger, J., Berkes, F., Hoor, P., Platt, U., Lelieveld, J., and Crowley, J. N.: Chemical and meteorological influences on the lifetime of NO₃ at a semi-rural mountain site during PARADE, *Atmos. Chem. Phys.*, 16, 4867–4883, <https://doi.org/10.5194/acp-16-4867-2016>, <https://www.atmos-chem-phys.net/16/4867/2016/>, 2016.

605 Sommariva, R., Cox, S., Martin, C., Borońska, K., Young, J., Jimack, P., Pilling, M. J., Matthaios, V. N., Newland, M. J., Panagi, M., Bloss, W. J., Monks, P. S., and Rickard, A. R.: AtChem, an open source box-model for the Master Chemical Mechanism, submitted, 2019.

Sulzer, P., Hartungen, E., Hanel, G., Feil, S., Winkler, K., Mutschlechner, P., Haidacher, S., Schottkowsky, R., Gunsch, D., Seehauser, H., Striednig, M., Jürschik, S., Breiev, K., Lanza, M., Herbig, J., Märk, L., Märk, T. D., and Jordan, A.: A proton transfer reaction-quadrupole interface time-of-flight mass spectrometer (PTR-QiTOF): high speed due to extreme sensitivity, *Int. J. Mass Spectrom.*, 368, 1–5, <https://doi.org/10.1016/j.ijms.2014.05.004>, 2014.

Tani, A., Hayward, S., and Hewitt, C. N.: Measurement of monoterpenes and related compounds by proton transfer reaction-mass spectrometry (PTR-MS), *Int. J. Mass Spectrom.*, 223–224, 561–578, [https://doi.org/10.1016/s1387-3806\(02\)00880-1](https://doi.org/10.1016/s1387-3806(02)00880-1), 2003.

610 Whalley, L. K., Edwards, P. M., Furneaux, K. L., Goddard, A., Ingham, T., Evans, M. J., Stone, D., Hopkins, J. R., Jones, C. E., Karunaharan, A., Lee, J. D., Lewis, A. C., Monks, P. S., Moller, S. J., and Heard, D. E.: Quantifying the magnitude of a missing hydroxyl radical source in a tropical rainforest, *Atmos. Chem. Phys.*, 11, 7223–7233, <https://doi.org/10.5194/acp-11-7223-2011>, <https://www.atmos-chem-phys.net/11/7223/2011/>, 2011.

Whalley, L. K., Stone, D., Bandy, B., Dunmore, R., Hamilton, J. F., Hopkins, J., Lee, J. D., Lewis, A. C., and Heard, D. E.: Atmospheric OH reactivity in central London: observations, model predictions and estimates of in situ ozone production, *Atmos. Chem. Phys.*, 16, 620 2109–2122, <https://doi.org/10.5194/acp-16-2109-2016>, <https://www.atmos-chem-phys.net/16/2109/2016/>, 2016.

Williams, J.: Organic trace gases in the atmosphere: an overview, *Environ. Chem.*, 1, 125, <https://doi.org/10.1071/EN04057>, 2004.

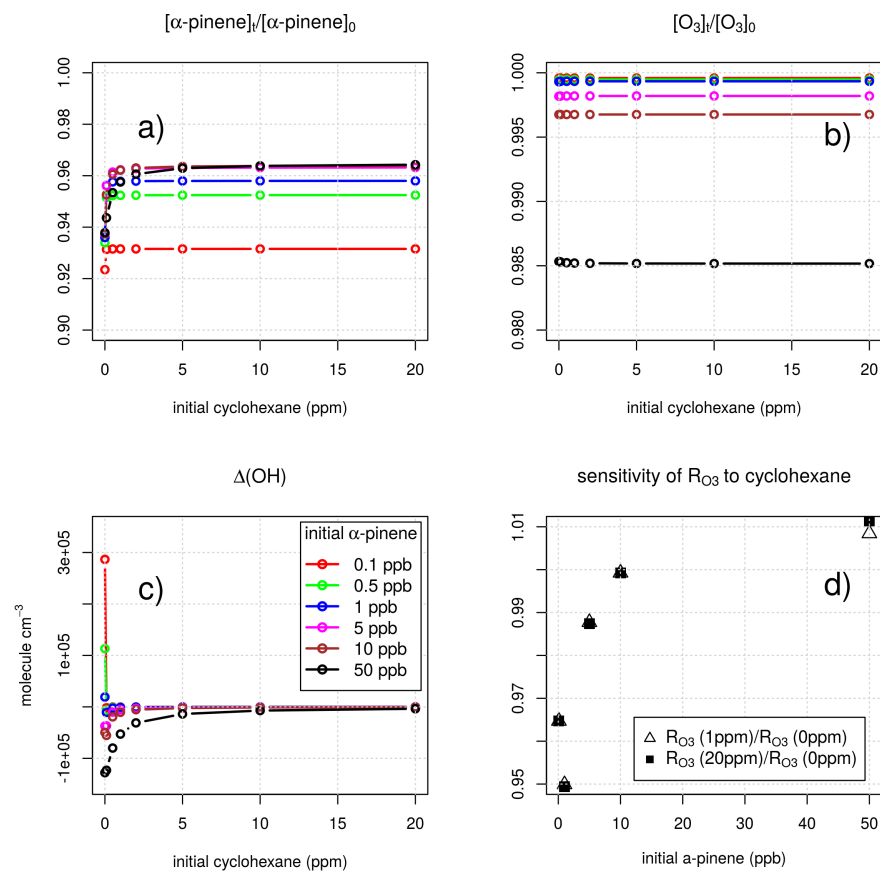


Figure 1. Modelled removal of α -pinene and O_3 (relative to their initial concentrations) as a function of cyclohexane level (a-b). Modelled difference between the initial and final concentrations of OH as a function of cyclohexane level (c). Sensitivity of modelled R_{O_3} to cyclohexane concentrations as a function of the initial α -pinene concentration (d).

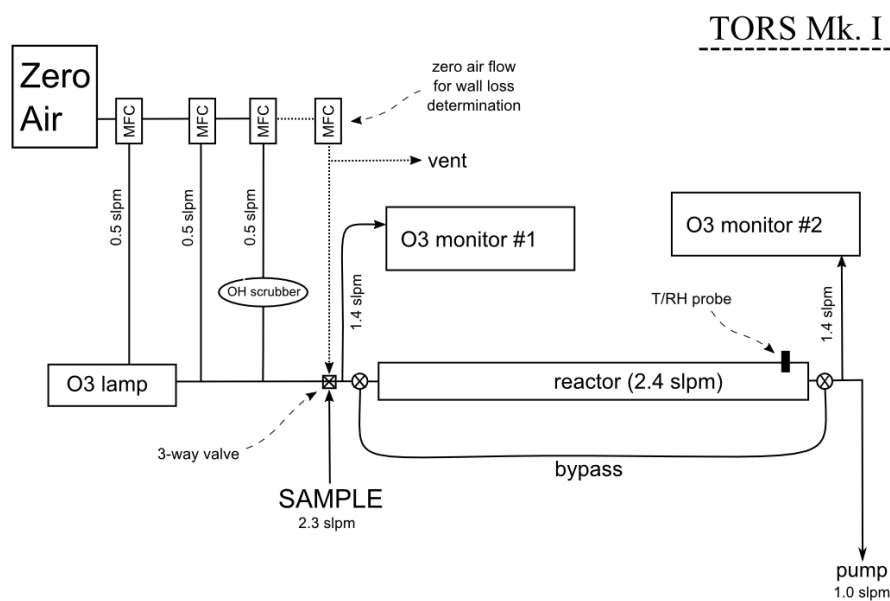


Figure 2. Diagram of the TORS instrument with typical flow settings (Sect. 4.3).

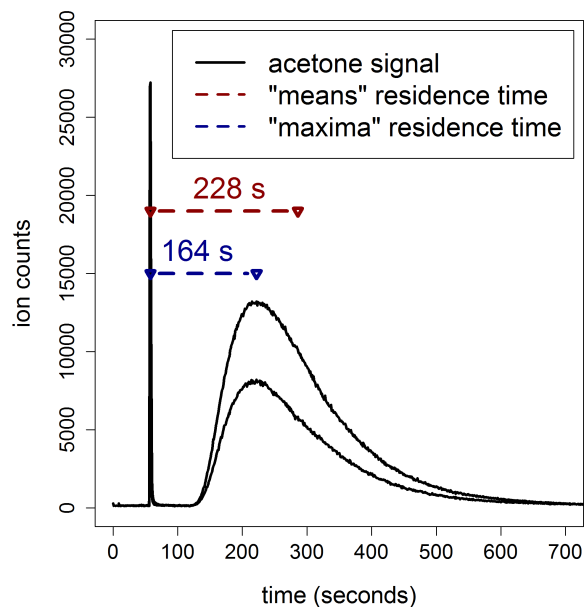


Figure 3. Two acetone double injection experiments used to estimate the residence time in the PTFE reactor for a flow rate of 1600 sccm. The “maxima” calculation uses the differences in time of the peak acetone signals; the “means” method uses the differences between the mean elapsed time of the two acetone signals.

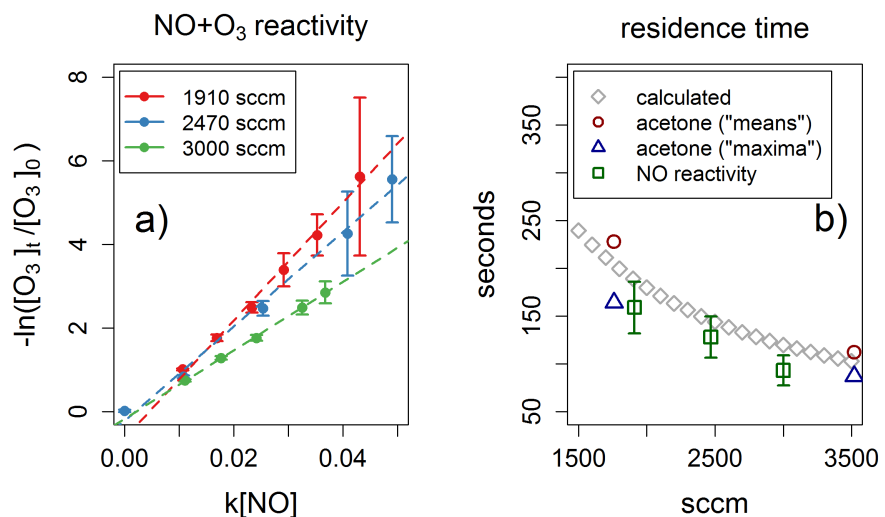


Figure 4. NO reactivity experiments (a). Residence times as a function of reactor flow, determined by three different methods (b). The results of the acetone injection method are taken from Fig. 3.

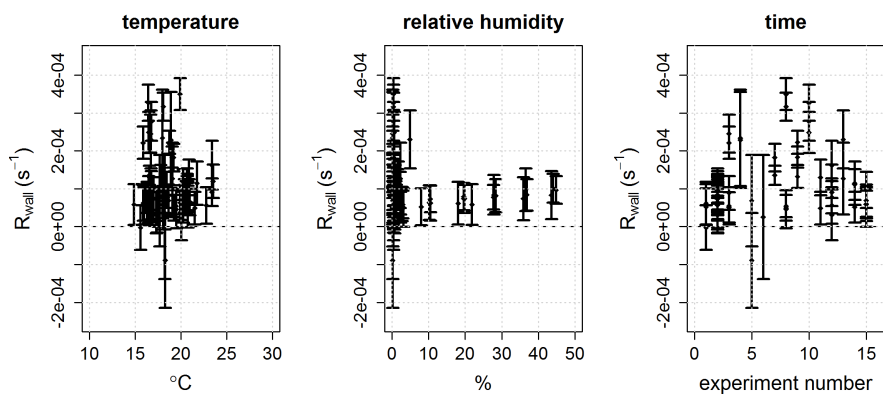


Figure 5. Mean and 2- σ standard deviation of the ozone wall loss (R_{wall}) in the PTFE reactor as a function of humidity, temperature and time. The data are taken from 15 experiments, with multiple determinations of R_{wall} per experiment, over a nine month period.

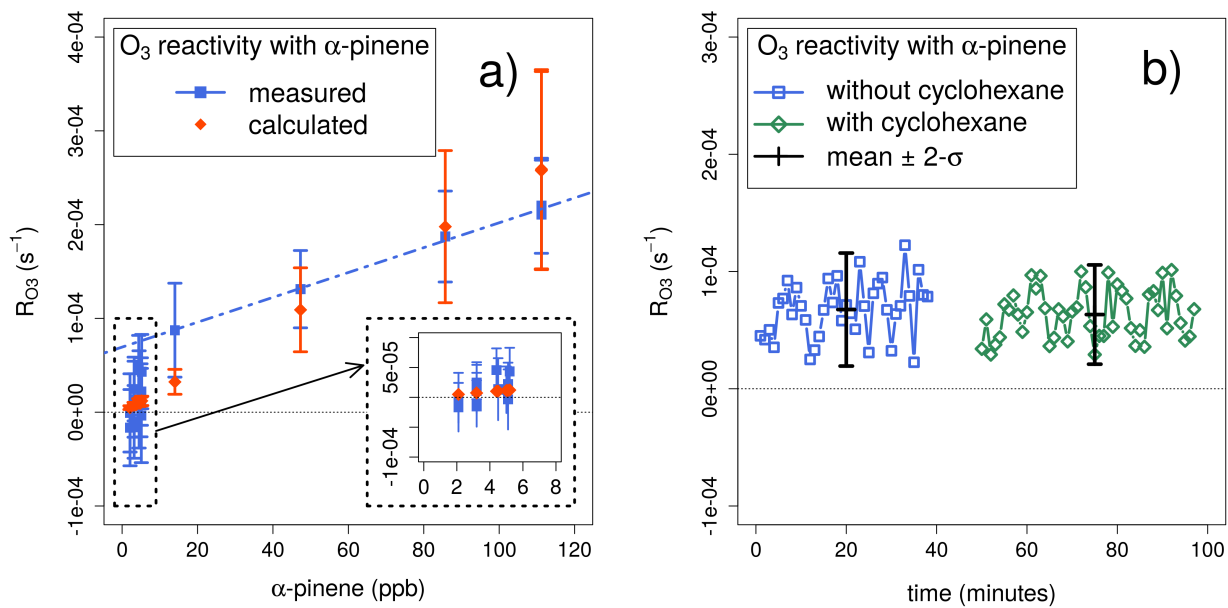


Figure 6. Measured and calculated mean ozone reactivities with α -pinene (a). Ozone reactivity with α -pinene measured with and without cyclohexane as OH scrubber (b). The blue dashed line (left panel) indicates the linear regression of the measured R_{O_3} values for α -pinene mixing ratios > 20 ppb.

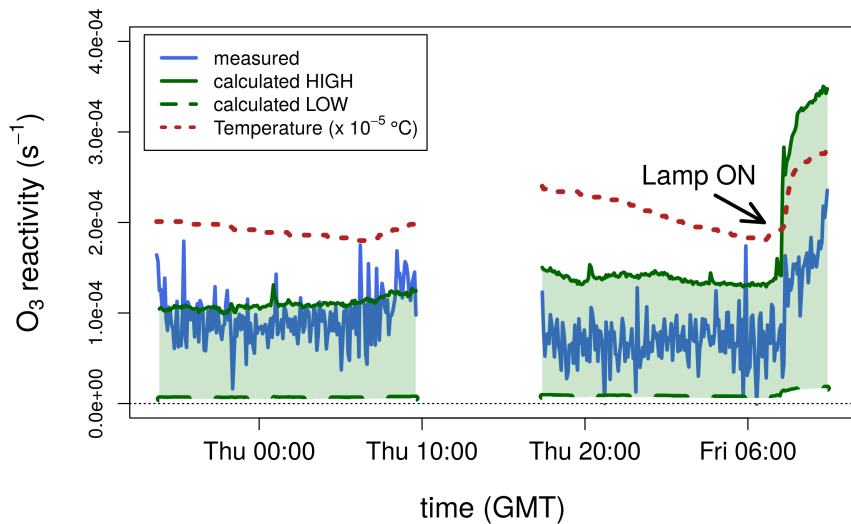


Figure 7. Measured ozone reactivity from 3 plants of lemongrass (*Thymus citriodorus*) in a Teflon bag, compared to the ozone reactivity calculated from measurements of BVOCs by PTR-MS. The temperature (in $^{\circ}\text{C}$) measured inside the bag is also shown. All data are averaged to 5 minutes.

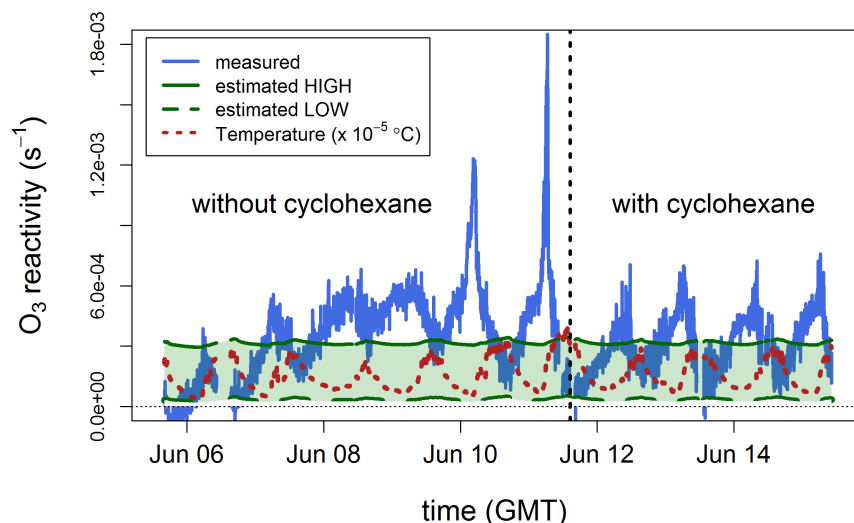


Figure 8. Measured ozone reactivity in the Winterbourne House and Garden glasshouse compared to ozone reactivity calculated from estimated BVOC concentrations. The temperature (in °C) measured inside the glasshouse is also shown. All data are averaged to 5 minutes.

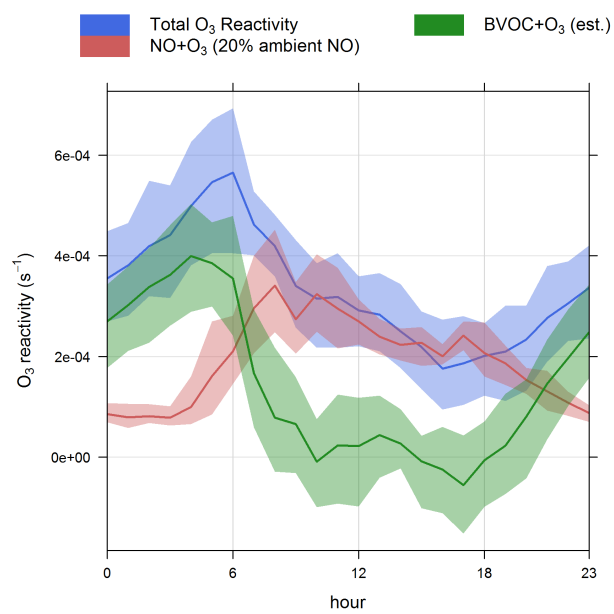


Figure 9. Diel averages of measured total ozone reactivity and estimated ozone reactivities with NO (R_{NO}) and BVOCs (R_{O3}).



Table 1. Rate coefficients of the reactions with ozone (k_{O_3} , in $\text{cm}^3 \text{molecule}^{-1} \text{s}^{-1}$), absolute ozone reactivities (R_{O_3} , in s^{-1}) and relative ozone reactivities (with respect to α -pinene) of selected BVOCs and inorganic compounds. The rate coefficients are from Atkinson et al. (2004, 2006) and calculated for standard conditions (298 K, 1 atm); the ozone reactivities are calculated for mixing ratios of 1 ppb.

Class	Species	k_{O_3}	R_{O_3}	relative R_{O_3}
hemiterpenes	isoprene	1.28×10^{-17}	3.15×10^{-7}	0.13
monoterpenes	α -terpinene	1.90×10^{-14}	4.68×10^{-4}	197.97
	β -ocimene	5.70×10^{-16}	1.25×10^{-5}	5.31
	myrcene	4.70×10^{-16}	1.16×10^{-5}	4.90
	limonene	2.20×10^{-16}	5.41×10^{-6}	2.29
	α -pinene	9.60×10^{-17}	2.36×10^{-6}	1
	β -pinene	1.89×10^{-17}	4.67×10^{-7}	0.20
	sabinene	8.30×10^{-17}	2.04×10^{-6}	0.86
	3-carene	4.90×10^{-17}	1.21×10^{-6}	0.51
	camphene	5.02×10^{-19}	1.24×10^{-8}	0.01
sesquiterpenes	β -caryophyllene	1.20×10^{-14}	2.96×10^{-4}	125.03
	α -farnesene	5.88×10^{-16}	1.45×10^{-5}	6.13
	α -copaene	1.50×10^{-16}	3.69×10^{-6}	1.56
	longifolene	5.00×10^{-19}	1.23×10^{-8}	0.01
inorganic	NO	1.89×10^{-14}	4.65×10^{-4}	196.56
	HO ₂	2.01×10^{-15}	4.96×10^{-5}	20.99
	NO ₂	3.52×10^{-17}	8.67×10^{-7}	0.37